OPTICAL MAGNETOMETER EMPLOYING ARTIFICIAL INTELLIGENCE FOR MAGNETIC FIELD IMAGING

SOFIA BROWN and IRINA NOVIKOVA
College of William and Mary

April 2022

Abstract

We combine a camera, an optical fiber, and artificial intelligence into a single optical magnetometer for magnetic field imaging. This novel combination provides enhanced spatial resolution, a mobile configuration, and efficient, unbiased data processing capabilities. The magnetometer is based on an undergraduate laboratory Faraday rotation apparatus (a glass rod surrounded by a solenoid), linked to a camera via a multimode optical fiber. To identify varying magnetic field strengths, an image classification algorithm analyzes the fiber output "speckle" patterns that result from different magnetically-induced changes in probe beam polarization. Initially, as we constructed and strengthened the algorithm, we simulated these polarization changes using a waveplate. Later, we replaced the waveplate with the glass rod and solenoid. Ultimately, we created a sensor with angular sensitivity of at least $\frac{1}{256}^\circ$, corresponding to magnetic fields of about 56 μT. Investigations are underway to check changes in polarization in the range of $\frac{1}{256}^\circ$ to $\frac{1}{4096}^\circ$, which would correspond to magnetic fields from 56 μT to 3 μT. In the future, we hope to replace the solenoid with a Rubidium vapor cell to create an atomic magnetometer with enhanced sensitivity.

1 Introduction

1.1 Background

Magnetic field sensors have a wide variety of NASA-related applications, making them an ongoing and prolific topic of inquiry within the institution. The uses of magnetometers range from structural health analysis of aerospace vehicles and weather prediction to heartbeat monitoring and weapon systems positioning.[1] As technology advances, the need for increasingly sensitive magnetometers continues to propel research on these devices. We propose a highly sensitive, optical magnetometer that boasts enhanced imaging capabilities and a mobile configuration. With these qualities, our device's applications will center on defect detection in metal components, which can be useful in areas like vehicle design and passenger safety.

1.2 Motivation and Theory

The quest for better sensitivity is ongoing in the field of magnetometry. Optical magnetometers enhance sensitivity by probing atoms in a magnetic field with light. They then use the atoms' and/or light's response to detect the field.

We will focus on one traditional type of optical magnetometer called a Faraday rotation magnetometer. This specific device relies on the change in polarization that light undergoes when

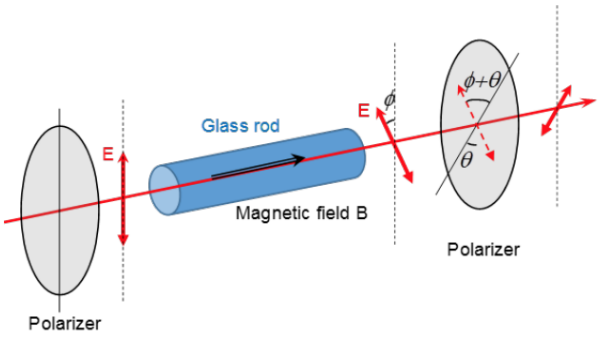

Figure 1: [2] A visualization of Faraday rotation, where light (red arrow) of a polarization θ traveling through a transparent medium subject to an external magnetic field, B will rotate by an angle, ϕ, proportional to B. Note that ϕ is much smaller than shown here.

interacting with atoms in a material that is exposed to a magnetic field. This phenomenon is called Faraday rotation. Specifically, in a transparent material like glass, a magnetic field, directed along the direction of light propagation will rotate the light's polarization by an angle ϕ, as shown in Figure 1.[2] This angle of polarization rotation is proportional to the magnetic field B according to

$$\phi = C_V B l, \tag{1}$$

where C_V is the Verdet constant, which depends on the material, and l is the length of the material along which the light propagates.

In the traditional setup, a magnetic field is imposed on the transparent material. A laser shines through this material and then encounters a polarizer on the other size. The change in laser polarization is then detected as a change in intensity using a photodiode at the output. Thus, the magnetic field is measured. Note, however, that for a reasonably sized magnetic field, the change in polarization is quite small. Indeed, in the setup shown in Figure 1, a magnetic field of 11.1mT leads to a polarization rotation on the order of 10^{-4} rad, or about $0.005°$.[2]

Figure 2: A comparison of the multimode fiber output "speckle" patterns for $0°$ (left) and $45°$ (right) polarization angles.

A significant drawback of this setup, however, is that using a photodiode as the sensing device does not provide any *spatial* resolution of the magnetic field. One solution is to replace the photodiode with a CCD camera to image the field.[3] The downside here is that adding a camera makes for a bulky sensor that would not be compatible with, say, chip-scale manufacturing.[4]

To solve this problem, we instead separated the camera physically from the Faraday rotation magnetometer using a multimode optical fiber. Fibers are inexpensive and will allow a portable, flexible device configuration. When light travels down a multimode fiber, its different modes scatter differently creating a kind of "speckle" pattern intensity profile. Thus, when the laser's polarization changes, its intensity does not change, but the speckle patterns do change, because of interference inside the fiber. Figure 2 shows a comparison of the speckle patterns for a $0°$ and $45°$ polarization. Therefore, we can use the differing speckle patterns to identify the beam polarizations corresponding to different magnetic fields. Furthermore, using a fiber eliminates the need for the polarizer that the conventional setup requires.

The drawback, though, is that the speckle patterns are complicated images. Also, when the change in polarization is small, as it is when magnetically-induced, the image features only change by a small amount, which is almost entirely undetectable visually. This problem in-

vites the use of artificial intelligence (AI). Borhani et al.[5] and Wang et al.[6] have shown that deep learning can be used to classify the "speckle patterns" that result from the propagation of an input image through a multimode fiber. We used a similar approach to identify the different speckle patterns that result from different magnetically-induced probe beam polarizations traveling through an MMF.

Ultimately then, we trained an image classification algorithm to recover the laser polarization from different speckle pattern images. This AI approach increases data processing power for rapid field measurement and analysis.

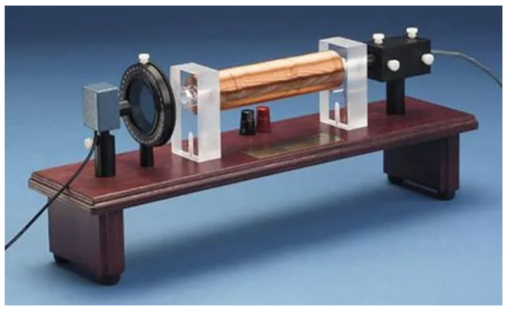

Figure 3: [2] TeachSpin's undergraduate Faraday rotation apparatus, consisting of, from right to left, a laser, a solenoid connected to a current supply and surrouding a glass rod, a polarizer, and a photodiode.

2 Experimental Design

For the Faraday rotation magnetometer, we used a modified version of TeachSpin Inc.'s undergraduate laboratory Faraday rotation apparatus, shown in Figure 3. The apparatus contains a 10cm long, 5mm diameter, SF-57 glass rod surrounded by a 15cm long solenoid that connects to a power supply. The value of C_V for the glass rod is 23 rad/T. For the solenoid, the calibration between input current, I, and magnetic field, B is

$$B = (11.1mT/A) \cdot I. \qquad (2)$$

For futher apparatus specifications, see the TeachSpin Faraday Rotation manual.[2]

For this work, we removed the laser, polarizer and photodiode that come attached to the apparatus. We then inserted the remaining part into our setup, as shown in Figure 4. Thus, our experimental setup is as follows: A 780.24 nm diode laser travels through a modified version of the TeachSpin Faraday rotation apparatus. After the light travels down the multimode fiber (MMF), a neutral density (ND) filter reduces the beam's intensitiy to a level appropriate for imaging. A CCD camera images the resultant beam profile. The images are then sent to the image classification algorithm. The

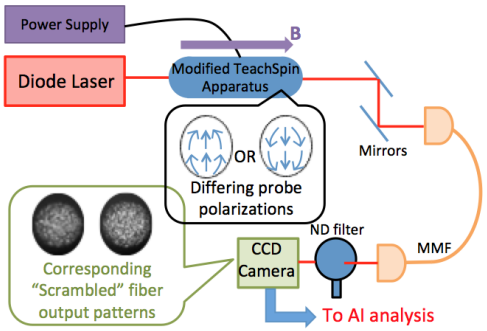

Figure 4: The experimental setup for the optical fiber-linked magnetometer using AI for magnetic field imaging.

MMF, ND filter, and CCD camera are all contained in a cardboard box to shield from temperature changes and ambient light. We also concluded that the laser power should remain constant during data acquisition and that a single image dataset should be taken within the same day to avoid significant drifting of the speckle patterns in time, which would skew algorithm performance.

After collecting the images, we rescaled them from 1024x1280 pixels to 256x320 pixels using interpolation. (This size was determined in previous work to be optimal for avoiding long algorithm run times without sacrificing algorithm

performance). We also normalized the images so that their pixel values fell between zero and one, taking care to avoid image saturation when recording data. Finally, we imposed a circular mask on each image. The mask was the size of the beam and blocked out the regions of the image outside the beam, thus ensuring that the algorithm only analyzed the actual speckle pattern during training.

3 Achieving Image Recognition

Preliminary work was done to establish baseline image recognition in our algorithm. We will describe the details of the algorithm in Section 4.1.

To achieve a functioning algorithm, we first used a waveplate to simulate the polarization rotation that a magnetic field would create. Thus, to start off, in our experimental setup (Figure 4), we had no Faraday apparatus or power supply, but rather, just a half waveplate. With this waveplate setup, we achieved angular sensitivity as low as $\frac{1}{4}^\circ$. We took 125 images each of 0 $^\circ$, $\frac{1}{8}^\circ$, $\frac{1}{4}^\circ$, $\frac{1}{2}^\circ$, and 1°. For each angle, the training set contained 100 images, and the testing set contained 25. A pause of 5 seconds separated each image capture. We trained on these images for 200 iterations.

The performance accuracies are shown in Table 1. The performance was highly accurate except in the $\frac{1}{8}^\circ$ case. A change of $\frac{1}{8}^\circ$ was 74% accurate, but this result is unreliable as the change in polarization is on the order of the waveplate's precision. Errors could easily have arisen here during waveplate rotation. Replacing the waveplate with the Faraday magnetometer avoided this problem later on since we could implement precise current values corresponding to a specific magnetic field. Thus, with the waveplate setup, we reached an angular sensitivity of $\frac{1}{4}^\circ$.

Training Polarizations	Testing Accuracy
0° vs. 1°	1
0° vs. $\frac{1}{2}^\circ$	0.86
0° vs. $\frac{1}{4}^\circ$	0.9
0° vs. $\frac{1}{8}^\circ$	0.74

Table 1: Image Classification Accuracies for changes in polarization of 1°, $\frac{1}{2}^\circ$, $\frac{1}{4}^\circ$, and $\frac{1}{8}^\circ$ using the waveplate.

4 Implementing a Faraday Magnetometer

4.1 The Image Classification Algorithm

For this work, we used a convolutional neural network (CNN) developed in MATLAB as our deep learning image classification platform. A CNN distinguishes images by assigning importance, or weight, to the images' distinguishing features. The network's structure mimics that of a human brain, with different layers connected by neurons.

The flow chart in Figure 5 is a visual representation of the CNN we built for this work. The algorithm consists of three convolutional layers, each followed by a normalization layer and a "pooling" layer. During the convolutional layers, the algorithm scans the image matrices using a "filter," a matrix of weights smaller than the image itself, which extracts the image's most important features. The normalization and pooling layers collect these features into smaller matrices that the algorithm categorizes. While this cycle repeats over many iterations, the algorithm assesses its categorizations for accuracy and updates its prediction to reach optimal classification. To further improve performance, the programmer may adjust the filter size and number of filters used in each layer. The "learning rate," or how fast the algorithm optimizes itself, can also be changed for best performance. In this work, we found an optimal learning rate of

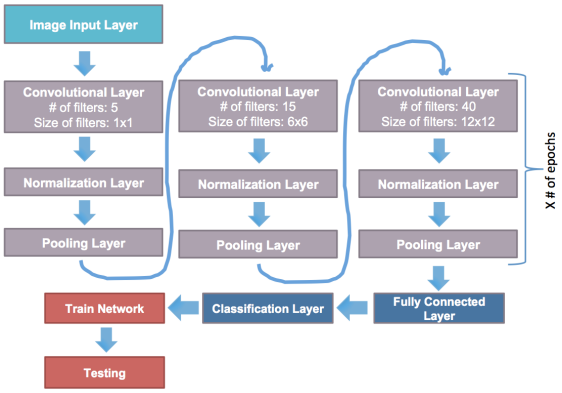

Figure 5: A flow chart representation of the image classification algorithm used in this work. Each colored box represents a layer in the neural network. Size and number of filters used in each layer are noted.

10^{-5}, which means that the algorithm updates the filter weights by 10^{-3} % of the classification error during each cycle. Learning rates fall between 0 and 1. Our very low value reflects the complexity of our image data.

In this work, we used "learning curves" to monitor the training process. These curves are plots of algorithm accuracy and loss versus training iteration. An ideal learning curve, shown in Figure 6 (left) will show accuracy increasing to 100% and loss decreasing to zero. Accuracy and loss behavior should more or less mirror each other. Plateauing accuracy and/or increasing loss, Figure 6, (right), indicate poor training.

The last layer of the classification process is the Testing layer. Here, the algorithm is fed new images that are similar to those it has been trained on to see how well it performs after training. The algorithm then outputs a performance accuracy, as a percent, which we use to assess overall classification success.

Helpful background information on convolutional networks can be found in the overview paper by Albawi et al.[7] Other more informal sources include webpages by Adit Deshpande[8]

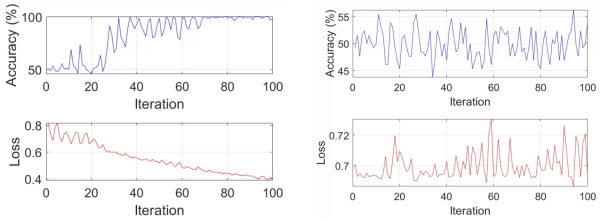

Figure 6: On the left is an example of a optimal learning curve, and the right is an example of a suboptimal learning curve. Plotted are training accuracy (top) and loss (bottom) vs. training iteration.

and Sumit Saha.[9]

4.2 Faraday Magnetometer Benchmark Angular Sensitivity Tests

Having concluded that our algorithm could distinguish different laser polarizations successfully, we replaced the waveplate in our setup with the Faraday magnetometer, as shown in Figure 4. We first created a calibration of laser polarization rotation vs. current supplied to the solenoid, and we used this calibration throughout the remaining work.

We conducted benchmark tests for angular sensitivity in the new setup to ensure that algorithm performance was comparable to when using the waveplate. We took images of $0°$, $0.5°$, $1°$, $1.5°$, and $2°$. As before, the training sets for each angle consisted of 100 images and the testing sets consisted of 25. A pause of 3 seconds separated each image capture, and trainings were conducted for 100 iterations. All possible combinations of angles were tested, and the training plots were ideal in all cases, with four examples shown in Figure 7.

Table 2 shows that the performance accuracy was 100% in all cases except two. Interestingly, these two cases still demonstrated ideal learning curves (Figure 7 top left and bottom right). From here, we can conclude that, so far, the algorithm can generally distinguish be-

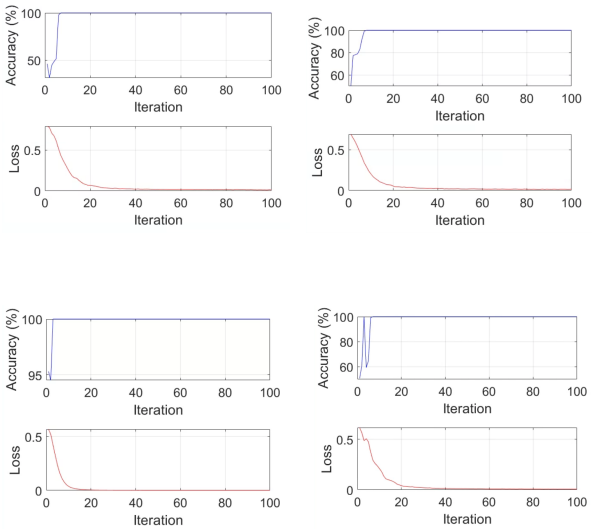

Figure 7: Learning Curves for determining benchmark angular sensitivity using the Faraday magnetometer. The top left plot shows training to distinguish between $0.5°$ and $1°$, the top right shows $1°$ and $1.5°$, the bottom left shows $1°$ and $2°$, and the bottom right shows $0°$ and $0.5°$.

Training Polarizations	Testing Accuracy
0 ° vs. 0.5 °	0.92
0 ° vs. 1 °	1
0 ° vs. 1.5 °	1
0 ° vs. 2 °	1
0.5 ° vs. 1 °	0.8
0.5 ° vs. 1.5 °	1
0.5 ° vs. 2 °	1
1 ° vs. 1.5 °	1
1 ° vs. 2 °	1
1.5 ° vs. 2 °	1

Table 2: Image Classification Accuracies for the benchmark Faraday magnetometer tests.

tween changes in polarization as small as half a degree.

4.3 Improving Angular Sensitivity

With these promising results, we tested the algorithm's response to smaller angles taken using the Faraday magnetometer setup. As with the waveplate, we tested differences in polarization of $\frac{1}{2}°$, $\frac{1}{4}°$, and $\frac{1}{8}°$. As shown in Table 3, the algorithm was 100% accurate in distinguishing a $\frac{1}{2}°$ change in polarization, as before. However, for a $\frac{1}{4}°$ change, it was only 66% accurate with 100 iterations, and for a $\frac{1}{8}°$ change, it was 84% accurate with 100 iterations. Interestingly, increasing the number of iterations to 200 changed the $\frac{1}{4}°$ accuracy to 74 % and *decreased* the $\frac{1}{8}°$ accuracy to 72%.

Interestingly, the training plots (Figure 8) were ideal in terms of accuracy. However, we

Training Polarizations	Number of iterations	Testing Accuracy (%)
0 ° vs. $\frac{1}{2}°$	100	1
0 ° vs. $\frac{1}{4}°$	100	66
0 ° vs. $\frac{1}{8}°$	100	84
0 ° vs. $\frac{1}{4}°$	200	74
0 ° vs. $\frac{1}{8}°$	200	72

Table 3: Image Classification Accuracies for Fractional Angles Using the Faraday Magnetometer.

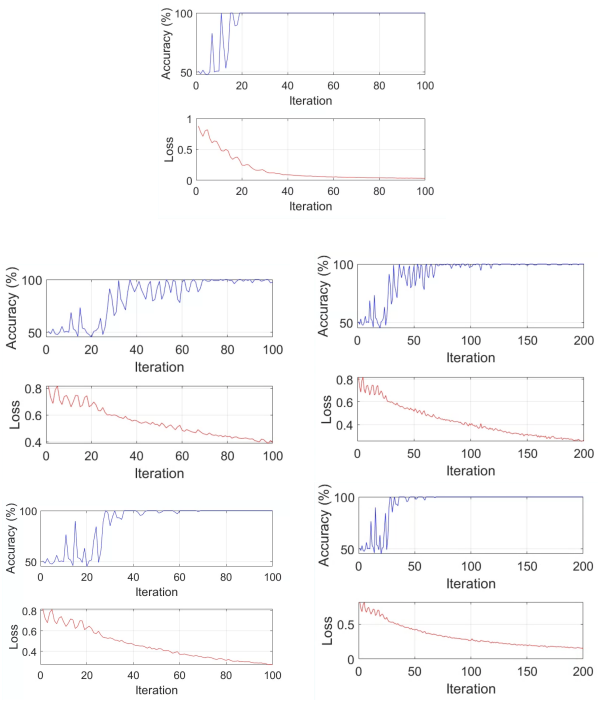

Figure 8: Learning Curves for determining angular sensitivity using the Faraday magnetometer. The topmost plot shows training to distinguish between $0°$ and $\frac{1}{2}°$, the second row shows $0°$ and $\frac{1}{4}°$ for 100 and 200 iterations (left and right, respectively), and the bottom row shows $0°$ and $\frac{1}{8}°$ for 100 and 200 iterations (left and right, respectively).

note that the loss did not decrease to zero, as it did in Figure 7. This may be contributing to the inconsistent accuracies.

To address these inconsistent results, we tried increasing the size of the testing and training sets to 500 images in each. We also ensured that images were placed into the testing and training sets randomly. These changes led to 100% accuracy in detecting a change in polarization as small as $\frac{1}{256}°$. The ideal learning curves and performance results are shown in Figure 9 and Table 4, respectively. Thus, we conclude that for these complicated speckle patterns, a training set larger than 100 images is essential to success.

Training Polarizations	Testing Accuracy
$0°$ vs. $\frac{1}{8}°$	1
$0°$ vs. $\frac{1}{16}°$	1
$0°$ vs. $\frac{1}{32}°$	1
$0°$ vs. $\frac{1}{64}°$	1
$0°$ vs. $\frac{1}{128}°$	1
$0°$ vs. $\frac{1}{256}°$	1

Table 4: Image classification accuracies for changes in polarization as small as $\frac{1}{256}°$ using the Faraday magnetometer.

When taking our images, we set a current of 7.3mA to correspond to the $0°$ polarization rotation. Using our current-to-polarization calibration of the apparatus, a current of 12.4mA corresponded to a polarization of $\frac{1}{256}°$. Using Equation 2, therefore, a $\frac{1}{256}°$ change in polarization corresponds to a change in magnetic field of about 56μT.

Investigations to test even smaller changes in magnetic field are underway. We are currently looking at changes in polarization from $\frac{1}{256}°$ to $\frac{1}{4096}°$, which would correspond to magnetic fields from 56 μT to 3 μT. So far, it is possible that the algorithm will be able to detect polarizations smaller than $\frac{1}{256}°$ without modification. Ultimatley, we would like to detect fields on the nano-Tesla scale.

5 Conclusion

Using our optical fiber-linked Faraday magnetometer, we detected a change in polarization as small as $\frac{1}{256}°$ with 100% accuracy. This sensitivity corresponds to a magnetic field of about 56μT.

Ultimately, our unique magnetometer design combines the structural and informational advantages of a fiber + camera setup with the efficient, unbiased data processing power of AI for enhanced spatial resolution and physical compactness. This approach provides a powerful

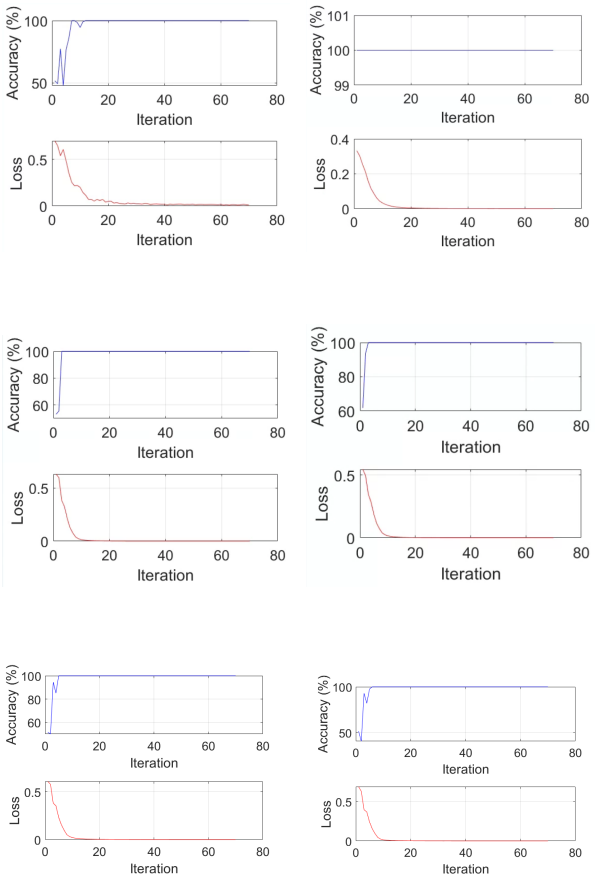

Figure 9: Learning Curves for determining angular sensitivity using the Faraday magnetometer. The top left plot: training to distinguish between $0°$ and $\frac{1}{8}°$; top right: $0°$ and $\frac{1}{16}°$; middle left: $0°$ and $\frac{1}{32}°$; middle right: $0°$ and $\frac{1}{64}°$.; bottom left: $0°$ vs. $\frac{1}{128}°$; bottom right: $0°$ and $\frac{1}{256}°$.

magnetic field sensing technique that will give researchers, engineers, and technicians enhanced information about an external magnetic field, with high sensitivity and speed. With its compactness and portability, our sensor is a versatile device, practical in settings that require mobility and small size. The main application will be in structural defects detection of, say, air and space vehicles, buildings and bridges, or pipelines and storage tanks.

Our sensor offers two exciting avenues for further improvements. A long-term possibility is to replace the glass rod and solenoid with a Rubidium atomic vapor cell. Using gaseous atoms will further improve sensitivity through the use of quantum light-matter interactions. If this implementation is successful, another possibility is to replace the atomic medium with a crystal. In this case, the device may instead be used to measure a high magnetic field, where an optical fiber would make for an ideal probe. With the compactness of our setup, using a crystal could also offer the option of a chip-scale device.

References

[1] Kitching, J., Knappe, S., and Donley, E.A."Atomic Sensors - A Review". In: *IEEE Sensors Journal* 11 (2011), pp. 1749-1758. DOI: 10.1109/JSEN.2011.2157679.

[2] https://www.teachspin.com/faraday-rotation

[3] Mikhailov, E. E., Novikova, I., Havey, M.D., Narducci, F. A. "Magnetic Field Imaging with Atomic Rb Vapor". In: *Optics Letters* 34 (2009), pp. 3529-3531. DOI: 10.1364/OL.34.003529.

[4] Kitching, J."Chip-Scale Atomic Devices". In: *Applied Physics Reviews"* 5 (2018), pp. 031302-1 - 031302-38. DOI:10.1063/1.5026238.

[5] Borhani, N., Kakkava, E., Moser, C., and Psaltis, D. "Learning to See through Multimode Fibers". In: *Optica* 5 (2018), pp. 960-996. DOI:10.1364/OPTICA.5.000960.

[6] Wang, P. and Di, J. ""Deep Learning-Based Object Classification through Multimode Fiber via a CNN-Architecture SpeckleNet". In: *Applied Optics* 57 (2018), pp. 8258-8263. DOI: 10.1364/AO.57.008258.

[7] Albawi, S., Mohammed, T. A., Al-Zawi, S. "Understanding of a Convolutional Neural Network". In: *IEEE International Conference on Engineering and Technology (ICET)* 2017, pp. 1-6. DOI: 10.1109/ICEngTechnol.2017.8308186.

[8] Deshpande, A. "A Beginners Guide to Understanding Convolutional Neural Networks." (2016) https://adeshpande3.github.io/A-Beginner%27s-Guide-To-Understanding-\Convolutional-Neural-Networks/

[9] Saha, S. "A Comprehensive Guide to Convolutional Neural Networks". *Towards Data Science* (2018). https://towardsdatascience.com/a-comprehensive-guide-to-\convolutional-neural-networks-\the-eli5-way-3bd2b1164a53